Materials Science Forum Vols. 794-796 (2014) pp 331-336
Online available since 2014/Jun/20 at www.scientific.net

doi:10.4028/www.scientific.net/MSF.794-796.331

Effect of Rolling on Mechanical Properties and Fatigue Behavior of an Al-Mg-Sc-Zr Alloy

Daria Zhemchuzhnikova[1a]*, Rustam Kaibyshev[1b]

[1]Belgorod State University, Pobeda 85, Belgorod 308015, Russia

[a]*zhemchuzhnikova@bsu.edu.ru, [b]rustam_kaibyshev@bsu.edu.ru

Keywords: Aluminium Alloys; Mechanical Properties; Fatigue; Hardening

Abstract. An aluminum alloy with a chemical composition of Al–6%Mg–0.35%Mn–0.2%Sc–0.08%Zr–0.07%Cr (in wt.) was rolled up to different reductions of 75, 88 and 95% at 360°C and at ambient temperature. The static mechanical properties and the high-cyclic fatigue (HCF) life were examined. It was shown that the hot rolling results in increased yield stress (YS) and ultimate tensile strength (UTS). However, ductility and fatigue limit of the hot rolled alloy and initial as-cast ingot are nearly the same. The combination of hot and cold rolling leads to significant improvement of tensile strength and fatigue resistance, while ductility tends to reduce with increasing the rolling reduction. The cold rolled alloy exhibits the endurance limit under fatigue conditions, while the alloy in the both as-cast and hot rolled conditions exhibits only fatigue strength. The effect of the deformation structure on the mechanical properties is discussed.

Introduction

It is known that aluminum alloys exhibit low fatigue resistance. The strengthening that could be achieved for the yield stress (YS) is not usually accompanied by corresponding improvements in fatigue properties [1]. The so-called fatigue ratio, which is relationship between the fatigue endurance limit determined in aluminum alloys at 5×10^8 cycles and the ultimate tensile strength (UTS), tends to decrease with increasing strength [1]. The fatigue ratio is moderate for non-heat treatable aluminium alloys. The endurance limit of these alloys achieves a value of 150 MPa at corresponding UTS value of 350 MPa and tends to be independent on further increase in the UTS [1]. In general, the fatigue failure of wrought aluminum alloys occurs through the formation of microcracks near surface followed by their coalescence and/or grow to macrocracks that propagate until the fracture [2,3]. The suppression of the formation of microcracks is critically important for attaining high fatigue resistance of non-heat treatable aluminum alloys [1,2]. There are two ways to hinder the formation of microcracks. The localization of strain in a limited number of coarse slip bands deteriorates fatigue resistance of Al-Mg alloys [1]. The microcracks nucleate at these bands where cyclic plastic deformation is significantly higher than the average (nominal) one [1-3]. The interaction of magnesium atoms with dislocations minimizes the formation of coarse slip bands, which play a role of cracklike flaws during fatigue [1-3]. Therefore, the fatigue performance of Al-Mg alloys with high Mg content could be superior if the crack initiation is delayed due to increased uniformity of dislocation slip. In addition, the uniformity of dislocation glide is achieved by nanoscale dispersoids [1,4]. This is the second effective way to enhance fatigue resistance [1].

Recently, high-strength Al-6%Mg-Sc alloys containing a dispersion of nanoscale particles of $Al_3(Sc,Zr)$ ($L1_2$) phase, which provide strong dispersion hardening, were developed [4,5]. The YS and UTS values of these alloys can be significantly increased by extensive strain hardening [6]. However, the fatigue properties of these alloys after rolling have not been insufficiently studied. The aim of the present paper is to investigate the effect of rolling on microstructure, mechanical properties and high cycle fatigue in an Al-Mg-Sc-Zr alloy.

Experimental Procedure

The alloy, denoted here as 1575C Al, with a chemical composition of Al-6%Mg-0.35%Mn-0.2%Sc-0.08%Zr-0.07%Cr (in wt. %), was manufactured by semi-continuous casting. The ingot was homogenized at 360°C for 12 h and cut into plates with dimension of 80 × 80 × 40 mm. These plates were hot rolled at 360°C to final thicknesses of ~ 10 mm with a total reduction of 75%. These samples are denoted as HR75. Part of these samples was subjected to subsequent cold rolled with reductions of 50 and 80% to final thicknesses of 5 and 2 mm, respectively. These samples are denoted as CR50 and CR80, respectively. A two-high mill with internal rollers 300 mm in diameter and 350 mm in length was used.

All mechanical tests were carried out at room temperature. The samples of the as-cast, HR75 and CR50 with a gage cross section of 3×7 mm^2 and a gage length of 25 mm were machined from the central areas of the plates with a gage length parallel to rolling direction (RD). The samples of the CR80 have a gage cross section of 1.5×3 mm^2 and a gage length of 12 mm. Tensile tests were performed using an Instron 5882 testing apparatus with an initial strain rate of ~ 10^{-3} s^{-1}. Samples for tensile test were prepared in accordance with ASTM E8/E8M-08 standard.

Fatigue tests were performed under ambient conditions using an Instron model 8801 servohydraulic system in tension. The dog-bone specimens, whose sizes were selected depending on the plate thickness in accordance with ASTM E466-07 standard, were cycled sinusoidally at a frequency of 25 Hz, using a minimum/maximum stress ratio R=0.1. The longitudinal sections of the specimens were parallel to the central axis of the ingot or the RD. The fatigue stress-number of cycles to failure curves were plotted with the data from the above tests.

The samples for electron back scattering diffraction (EBSD) and transmission electron microscopy analyses were cut from the central areas of the ingots and plates along the central line of the ingot and parallel to the RD, respectively. The details of sample preparation for structural characterization have been reported in a previous work [7]. The black and white lines in the EBSD maps indicate the high-angle boundaries (HABs) and low-angle boundaries (LABs) with misorientations of $\theta \geq 15°$ and $2 \leq \theta < 15°$, respectively. The dislocation densities were evaluated using a JEM-2100 transmission electron microscope by a method described in previous work [8].

Results and Discussion

Microstructures. The microstructure of the as-cast and HR75 alloys was previously described in work [7]. It is necessary to emphasize that the initial microstructure of the–1575C Al consists of coarse grains having round shape with an average size of about 22 μm (Fig. 1a & a'). Microstructure of HR75 samples consists of initial grains elongated along rolling direction, well-defined subgrain structure and moderate density of lattice dislocations (Fig. 1b & b', Table 1) [7]. The deformation microstructure of CR50 samples contains lamellar grains with an average thicknesses of ~ 1,2 μm (Fig. 1c & c'). The deformation bands outlined by the LABs are seen within these grains and an evidence for shear banding can also be detected (Fig. 1c). The cold rolling with a reduction of 50% resulted in an increase in lattice dislocation by a factor of 10; the fraction of the HABs and their average misorientation attain ~ 35% and 20^o, respectively (Fig 1c', Table 1).

The deformation microstructure of CR80 samples is essentially the same (Fig. 1d & d', Table 1). The increase in the reduction of the cold rolling promotes the shear banding. The elongated grains are subdivided by the shear bands oriented at ±30-40° to the RD [9,10]. The cold rolling provides increased density of the lattice dislocations (~ 6.4×10^{14} m^{-2}) (Fig. 1d & d', Table 1).

Mechanical properties. Engineering stress-strain curves and the values of the YS, UTS and total elongation-to-failure (δ) are presented in Figure 2 and Table 2. The as-cast alloy exhibits the lowest tensile strength of ~360 MPa (Fig. 2). The so-called type A serrated flow, which is attributed to the Portevin Le Chatelier (PLC) effect [7,11], takes place. This type of serration results from the repetitive continuous propagation of deformation bands from one end of the gauge to the other [11].

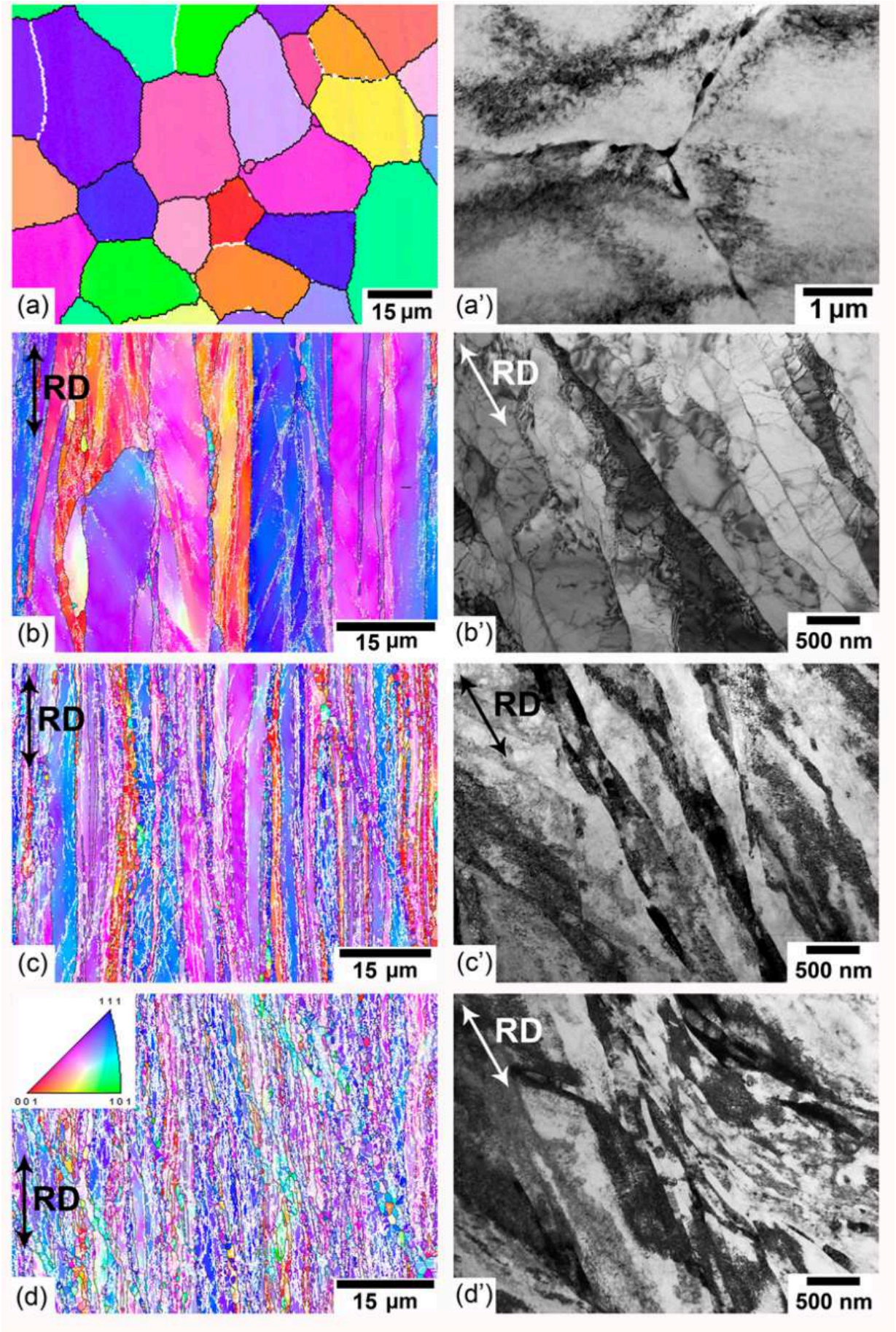

Fig. 1. Microstructure of the 1575C Al in the (a, a') as-cast state and after rolling for different thickness reductions: (b, b') HR75; (c, c') CR50; (d, d') CR80.

Table 1. The measured values of the average misorientation angle (Θ), the fraction of high angle boundaries (f_{HABs}) and the density of lattice dislocations (ρ) of the 1575C Al in the as-cast and rolled states.

Condition	Θ [deg]	f_{HABs} [%]	ρ [m^{-2}]
As-cast state	38	87	3×10^{12}
HR75	10	20	4×10^{13}
CR50	20	35	3.5×10^{14}
CR80	16	32	6.4×10^{14}

The hot rolling increases the YS from 225 to 295 MPa, the UTS from 360 to 450 MPa and the elongation-to-failure from 12% to 20 (Fig. 2a, Table 2). The HR75 alloy exhibits type B serrations (Fig. 2a). This type of jerky flow corresponds to a hopping propagation of localized bands [7,11].

As expected, the combination of hot and cold rolling leads to a significant increase in the strength and a reduction in ductility (Fig. 2a, Table 2). The CR80 alloy exhibits the highest UTS value of ~ 560 MPa, the elongation-to-failure is ~ 8%. The CR50 and CR80 samples show evidence of type A serrations [11] (Fig.2a).

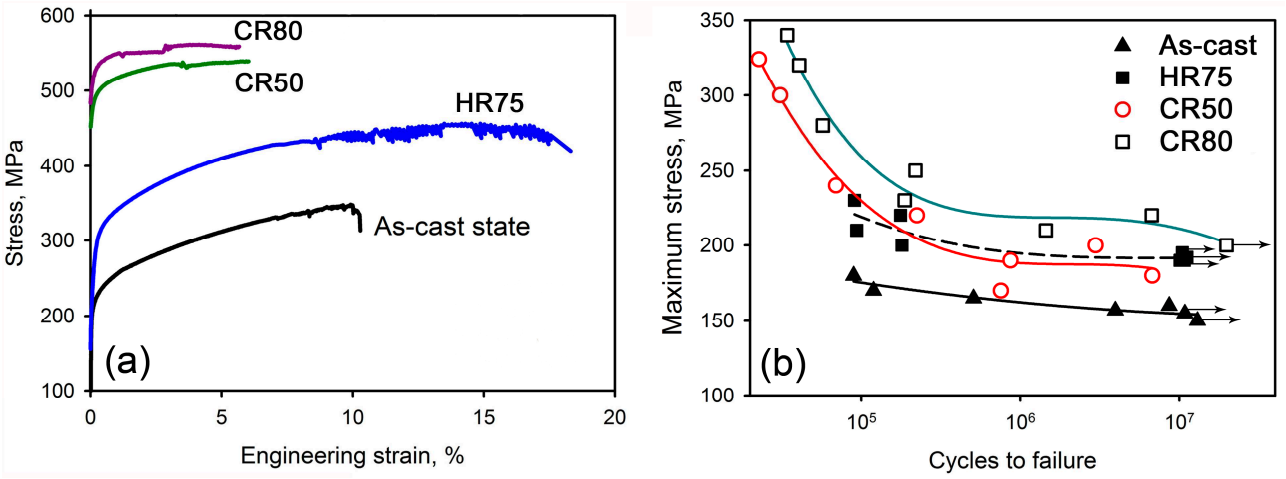

Fig. 2. Engineering stress–strain (a) and maximum stress-fatigue life (b) curves for all states of the 1575C alloy. Arrows represent run-out tests.

Figure 2b shows the stress–strain curves for all states of the 1575C Al. The fatigue limit is not well observed, which is typical of majority of aluminium alloys [12]. Therefore, the fatigue endurance limit on 10^7 cycles could be determined to evaluate high cycle fatigue life (Table 2) [12]. In general, increase in the UTS leads to increase in the fatigue strength [12-14], but fatigue ratio tends to decrease with increasing UTS (Table 2). The highest fatigue strength of ~210 MPa was observed in the CR80. The values of fatigue strengths of HR75 and CR50 alloys are approximately the same, i.e., ~ 180 MPa and ~190 MPa, respectively (Fig. 2b, Table 2). However, the cold rolling after hot rolling increases the fatigue resistance in low cycle range (cycles to failure $\leq 10^5$), significantly (Fig. 2b). It is worth noting that the S-N curves of cold rolled alloys exhibit the knees, while the as-cast and HR75 alloys display a continuously reduced stress-life response with increasing number of cycles.

Fractographic observation after fatigue. The SEM fractographs of the fracture surfaces of the alloy in the as-cast condition and after rolling are shown in Fig. 3. Numerous microcracks start to propagate from the specimen surface of the as-cast alloy along numerous cleavage planes (Fig. 3a). Numerous fatigue fracture surfaces are faceted and do not exhibit fatigue striations (Fig.3a). The crack growth generally occurs by transgranular fracture and is temporally arrested within interiors

of separate grains; short fatigue striations can be observed (Fig. 3a). In contrast, the restricted number of microcracks evolves and they propagate in ductile manner in the HR75 alloy. Continuous striations are observed (Fig. 3b) that is indicative that crack propagation is hindered in grain interior. The cracks propagate along planar grain boundaries. In the CR50 alloy, the fatigue fracture occurs in the essentially same manner (Fig. 3c). However, the resistance of grain interiors against crack propagation is higher that leads to the formation of numerous secondary cracks. The intergranular fracture impairs the fatigue resistance. In the CR80 alloy, the clearly defined striations are rarely observed (Fig. 3d). It seems that cracks may be effectively arrested in grain interiors. The striation-forming mode is changed to ductile intergranular fracture and dimple fracture in grain interiors. Thus, extensive rolling makes nearly unable propagation of fatigue cracks within grains, but facilitates intergranular fracture. As a result, there is no strong correspondence between the endurance limit and the UTS; the fatigue ratio decreases with increasing the UTS.

Table 2. Mechanical properties of the 1575C Al alloy in as-cast state and after rolling for different thickness reductions: the yield stress ($\sigma_{0.2}$), the ultimate tensile strength (σ_B), the total elongation-to-failure (δ) and the fatigue strength (σ_f)

Condition	$\sigma_{0.2}$, MPa	σ_B, MPa	δ, %	σ_f*, MPa	Fatigue ratio σ_f*/ σ_B
As-cast state	225	360	12	155	0.43
HR75	295	450	20	190	0.42
CR50	495	545	9	180	0.33
CR80	520	560	8	210	0.375

*maximum fatigue stress on the basis of 10^7 cycles

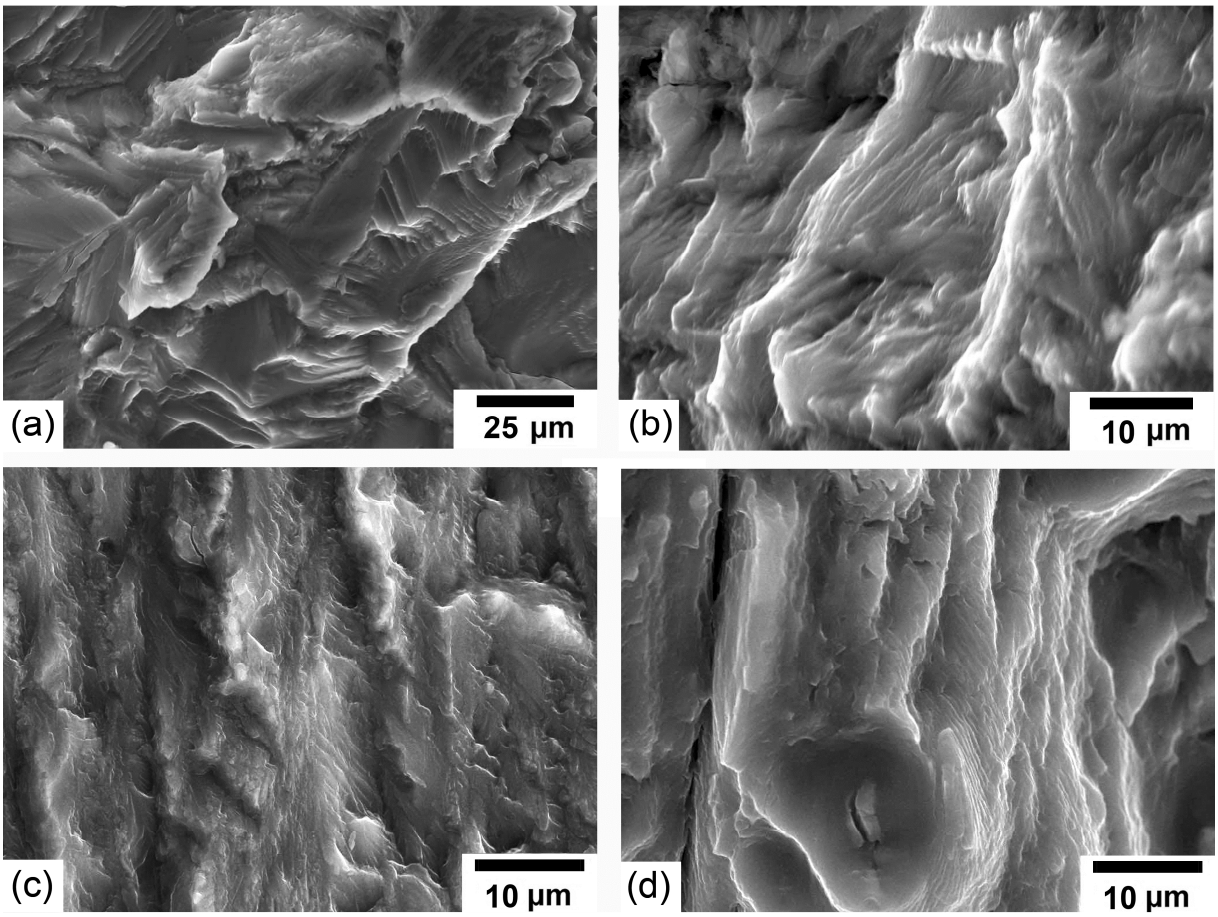

Fig. 3. Fracture surfaces of the fatigue specimens fractured after 10^7 cycles: (a) as-cast; (b) HR75; (c) CR50; (d) CR80.

Summary

The microstructures and the mechanical properties including the fatigue behavior of Al–6%Mg–0.35%Mn–0.2%Sc–0.08%Zr (in wt. %) alloy in the as-cast condition and after hot and cold rolling were examined.

1. The hot and cold rolling of the 1575C Al leads to an elongation of the initial grains, deformation banding and increased dislocation density.
2. The hot rolling results in increases in the yield stress from 225 to 295 MPa, the ultimate tensile strength from 360 to 450 MPa and the elongation-to-failure from 12% to 20%. The cold rolling with total reductions of 88% and 95% leads to increase of the yield stress to 495 MPa and 520 MPa, the ultimate tensile strength to 545 MPa and 560 MPa, respectively. The elongation-to-failure decreases to ~ 8% for the both cold rolled alloys.
3. The fatigue strength at 10^7 cycles of the as-cast alloy can be increased by 23% due to hot rolling and 35% due to combination of hot and cold rolling. The cold rolled alloys exhibits the "knees", while the as-cast and hot rolled states of alloy display a continuously reduced stress-life response with increasing number of cycles.
4. The fatigue ratio tends to decrease with increasing the ultimate tensile strength due to the fact that extensive rolling hinders crack propagation within grains, but facilitates intergranular fracture.

References

[1] I.J. Polmear, Light Alloys. From traditional alloys to nanocrystals. 4th ed., Butterworth-Heinemann/Elsevier, UK, 2006.

[2] W. F. Hosford. Mechanical Behavior of Materials. Cambridge University Press, New York, 2005, p.279.

[3] ASM Handbook, vol. 19, Fracture and Fatigue, ASM, Materials Park, OH, 1996.

[4] J. Røyset, N. Ryum, Inter. Mater. Rev. 50 (2005) 19-44.

[5] Yu.A. Filatov, V.I.Yelagin, V.V. Zakharov, Mater. Sci. Eng. A 280 (2000) 97.

[6] R. Kaibyshev, A. Mogucheva, A. Dubyna, Mater. Sci. For. 706-709 (2012) 55-60.

[7] D. Zhemchuzhnikova, A. Mogucheva, R. Kaibyshev. Mater. Sci. Eng. A 528 (2013) 132–141.

[8] R. Kaibyshev, K. Shipilova, F. Musin, Y. Motohashi, Mater. Sci. Eng. A 396 (2005) 341–351.

[9] P.J. Hurley, F.J. Humphreys, Acta Mater. 51 (2003) 1087–1102.

[10] Q. Liu, D. Juul Jensen, N. Hansen. Acta Mater. 46 (1998) 5819–5838.

[11] H. Halim, D.S. Wilkinson, M. Niewczas, Acta Mater. 55 (2007) 4151–4160.

[12] A. Vinogradov, A. Washikita, K. Kitagawa, V.I. Kopylov, Mater. Sci. Eng. A 349 (2003) 318-326.

[13] Y. Estrin, A. Vinogradov, Intern. Journal of Fatigue 32 (2010) 898–907.

[14] P. Cavaliere. Intern. Journal of Fatigue 31 (2009) 1476–1489.

Aluminium Alloys 2014 - ICAA14
10.4028/www.scientific.net/MSF.794-796

Effect of Rolling on Mechanical Properties and Fatigue Behavior of an Al-Mg-Sc-Zr Alloy
10.4028/www.scientific.net/MSF.794-796.331

DOI References
[4] J. Røyset, N. Ryum, Inter. Mater. Rev. 50 (2005) 19-44.
http://dx.doi.org/10.1179/174328005X14311
[5] Yu.A. Filatov, V.I. Yelagin, V.V. Zakharov, Mater. Sci. Eng. A 280 (2000) 97.
http://dx.doi.org/10.1016/S0921-5093(99)00673-5
[7] D. Zhemchuzhnikova, A. Mogucheva, R. Kaibyshev. Mater. Sci. Eng. A 528 (2013) 132-141.
http://dx.doi.org/10.1016/j.msea.2012.12.017
[8] R. Kaibyshev, K. Shipilova, F. Musin, Y. Motohashi, Mater. Sci. Eng. A 396 (2005) 341-351.
http://dx.doi.org/10.1016/j.msea.2005.01.053
[9] P.J. Hurley, F.J. Humphreys, Acta Mater. 51 (2003) 1087-1102.
http://dx.doi.org/10.1016/S1359-6454(02)00513-X
[10] Q. Liu, D. Juul Jensen, N. Hansen. Acta Mater. 46 (1998) 5819-5838.
http://dx.doi.org/10.1016/S1359-6454(98)00229-8
[11] H. Halim, D.S. Wilkinson, M. Niewczas, Acta Mater. 55 (2007) 4151-4160.
http://dx.doi.org/10.1016/j.actamat.2007.03.007
[12] A. Vinogradov, A. Washikita, K. Kitagawa, V.I. Kopylov, Mater. Sci. Eng. A 349 (2003) 318326.
http://dx.doi.org/10.1016/S0921-5093(02)00813-4
[13] Y. Estrin, A. Vinogradov, Intern. Journal of Fatigue 32 (2010) 898-907.
http://dx.doi.org/10.1016/j.ijfatigue.2009.06.022